Fuel 342 (2023) 127805

Contents lists available at ScienceDirect

Fuel

journal homepage: www.elsevier.com/locate/fuel

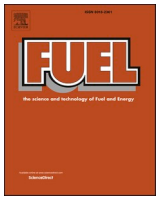

Full Length Article

On the effectiveness of metal particle combustion performance and implications to Martian missions

Quan Tran [a], Neil Vaz [a], Michelle L. Pantoya [a,*], Igor Altman [b,*]

[a] Department of Mechanical Engineering, Texas Tech University, Lubbock, TX 79424, USA
[b] Combustion Sciences and Propulsion Research Branch, Naval Air Warfare Center Weapons Division, China Lake, CA 93555, USA

ARTICLE INFO

Keywords:
Bomb calorimeter
Magnesium combustion
Metal powders
Condense-luminescence
Metal combustion modeling

ABSTRACT

There is a natural abundance of carbon dioxide in the Martian atmosphere that can oxidize magnesium fuel. Combustion of magnesium carried from Earth is considered as a potential propulsion process for Mars Ascent Vehicles. Other space exploration missions would benefit from magnesium combustion and thus sparked motivation to resolve puzzles in existing models for metal combustion. Harnessing all the chemical potential energy available in a metal particle will optimize power generation capabilities and payload demands. Here we design experiments to quantify metal combustion completeness, an important parameter that characterizes propulsion performance. Results show reduced energetic performance of magnesium combustion is directly related to the unavoidable occurrence of unburnt metal encapsulated in the combustion products caused by condense-luminescence. The new data provide insight into the advanced physics controlling metal particle combustion. The analyses suggest a path to improve magnesium energetic output by controlling radiative loss.

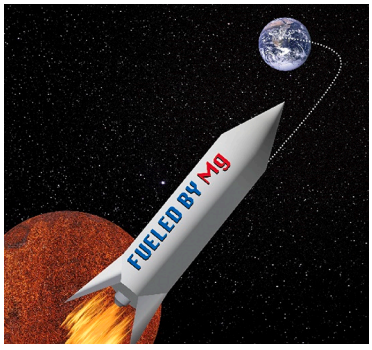

1. Introduction

Optimizing the energy generated from metal particles in propulsion applications requires a deep comprehension of various processes involved in metal combustion [1,2]. Advancing metal particle combustion to harness greater chemical potential energy requires detailed predictive models describing the particle combustion system. In the current literature devoted to metal particle combustion, there are gaps in understanding that prevent accurate process integration into global numerical models capable of predicting the system behavior.

Traditionally, metal particles such as magnesium (Mg), aluminum (Al), and boron (B) are used as additives to solid fuels to increase the system energy density, and, therefore, the rocket thrust. Although B has a higher energetic potential compared with Mg and Al, both Mg and Al

* Corresponding authors.
E-mail addresses: michelle.pantoya@ttu.edu (M.L. Pantoya), igor.altman2.civ@us.navy.mil (I. Altman).

https://doi.org/10.1016/j.fuel.2023.127805
Received 11 October 2022; Received in revised form 18 January 2023; Accepted 10 February 2023
Available online 14 February 2023

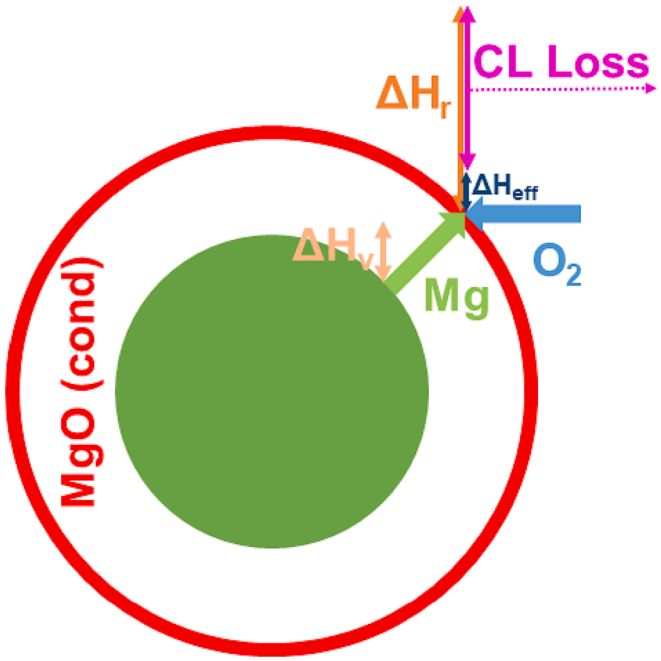

Fig. 1. Sketch illustrating the energy deficit for Mg particle vapor-phase combustion. Evaporation of Mg (shown in green color) requires energy of evaporation, ΔH_v. As a result of the reaction with oxygen (shown in blue color) that releases energy of ΔH_r, the condensed magnesia (shown in red color) is formed. In the case of significant CL radiative loss, the effective heat release ΔH_{eff} is not enough to sustain Mg evaporation.

exhibit better combustibility and are therefore mostly used in propulsion formulations. The best visually burning Mg powder has a lower energy density than Al, so Mg can often act as a combustion enhancer rather than the main metal fuel [3,4].

There is, however, a niche propulsion application, in which Mg would be the best metal fuel providing the highest overall mission performance [5]. The application originates from the growing interest in exploring Mars that requires Mars Ascent Vehicle (MAV) development. The uniqueness of using Mg in a MAV is related to the fact that the Martian atmosphere is made up almost entirely of carbon dioxide (CO_2) that is commonly considered an extinguishing agent, but is a good oxidizer for Mg [5]. The natural abundance of an oxidizer, and, therefore, no need to bring the oxidizer from Earth justifies possible advantages of the Mg-CO_2 propulsion system compared to traditional highly toxic propellants such as those containing hydrazine that are carried through space to Mars [6]. The essential conditions of using the Mg-CO_2 system is the completeness of Mg combustion that provides the maximum energy utilization. Harnessing energy from Mg combustion could expand the types of missions for which the metal-based propulsion would be beneficial.

The experimental studies of Mg-CO_2 combustion introduced a viable combustor configuration to support the process [7,8]. At the same time, the new perspective on the physics of metal combustion [9] poses the question on the possibility of complete combustion in principle and considers optimization strategies to fully yield all the metal's chemical potential energy. With regard to Martian missions, questions about completeness of combustion become crucial for mankind to optimize a propulsion system that would support expansion to Mars.

Historically, metal particle combustion concepts were adapted from hydrocarbon combustion models [10,11] that conditioned their current deficiencies [9]. Limited attention has been given to the important physical phenomena peculiar to metal combustion. In particular, in the case of volatile metal combustion, when the final products are nano-oxides, the condensation energy can be dissipated as light emission in the process called condense–luminescence (CL) [12]. As a result, the condensation energy released during nano-oxide formation can be lost in the energy balance of a burning particle [13]. Due to the condensation energy being a substantial part of the total heat of combustion, the loss of condensation heat leads to an energy deficit in the common metal particle combustion concept [9]. Fig. 1 illustrates the energy balance deficit of Mg particle combustion. At significant CL loss, the effective energy released in the reaction zone is not enough to sustain evaporation of Mg.

A possible way to resolve the energy-deficit related issue sketched in Fig. 1 and sustain steady-state metal particle combustion is to introduce an additional process that would compensate for the energy shortage. The process is the partial condensation of gaseous metal oxide on the surface of a burning metal particle in the particle combustion model [9,13]. That surface condensation is possible due to the particle temperature being lower than that of gaseous species. The heat released in partial condensation process may compensate for the condense-luminescent radiative energy loss. Although inclusion of partial condensation for the steady-state combustion looks compelling, its importance for accurate process modeling requires experimental evidence before revisiting existing models. At the same time, the condensation of gaseous metal oxide on the burning particle surface is experimentally challenging to directly observe. However, global characteristics of metal suspension combustion can infer micro-scale processes at the particle interface, such as condensation of gaseous metal oxides on the burning particle surface.

Here, experiments are designed to support the concept of the occurrence of gaseous metal oxide condensation on the burning particle surface. Two major experiments are performed, namely, 1) combustion of magnesium (Mg) powder suspension in a closed bomb calorimeter, and 2) differential scanning calorimetry (DSC) analysis of post-bomb combustion products. The purpose of the coupled bomb calorimetry and DSC experimental plan is to demonstrate the existence of unburnt metal encapsulated in the condensed oxide products collected after metal powder combustion within the calorimeter bomb. The occurrence of the metal core within the oxide shell from products of Mg combustion is only possible in the case of gaseous oxide condensation on the metal particle surface. Thus, the inferred partial gaseous oxide condensation that leads to the incompleteness of Mg combustion quantified in this work should guide further development of the corresponding propulsion systems for exploring Mars.

2. Methods

2.1. Materials

The Mg (99.9+% purity) powders were supplied by US Research Nanomaterials, Inc. (Houston, TX, USA) with two characteristic nominal Mg diameters of 10 μm and 100 μm (Stock # 1060, CAS# 7439-95-4). The porous medium used to suspend the powder in the bomb calorimeter was a starch-based material composed of poly-carbohydrates, including corn and potato starches. The porous poly-carbohydrate (PP) microstructure provides a readily combustible medium to disperse the powder and simulates powder suspensions [12,14].

2.2. Bomb calorimetry

Bomb calorimeter experiments were performed for the intrinsic measurement of heat of combustion, ΔH_c, using a Parr 6400 Automatic Isoperibol Calorimeter (Parr Instrument Co.). The details of the experimental setup are described by Tran et al. [14] and summarized here. All powder samples were measured at ~0.05 g and the porous PP medium was held constant at 0.10 g. The powder was dispersed in the PP medium, and the combined sample placed in a boron nitride crucible inside an 1138 Oxygen Combustion Vessel (Parr Instrument). The experimental technique used a PP medium to effectively suspend the powder during combustion. The ΔH_c was determined by combusting the sample

Table 1
Results for the heat of combustion, ΔH_c. The average values of ten experiments and the combustion completeness are presented with the standard deviations.

Mg Sample	10 μm	100 μm
Measured ΔH_c, kJ/g	23.46 ± 0.66	23.44 ± 0.92
Combustion Completeness, η, %	94.9 ± 2.7	94.8 ± 3.7

with excess oxygen at a pressure of 30 atm and subtracting the energy content of the PP dispersing media. Ten combustion experiments per each Mg size were performed.

The bomb calorimetry technique coupled with suspending the metal powder using the PP porous medium had been shown to produce heat of combustion of aluminum (Al) close (within the experimental error of about 2 %) to theoretical predictions that confirmed the completeness of Al combustion in the experiment [14].

2.3. Differential scanning calorimetry (DSC)

Thermal equilibrium analyses using DSC of post-bomb products and pre-burn (pure Mg) powders were performed. The purpose of these experiments was to (1) quantify incomplete Mg powder combustion obtained from post-bomb calorimetry tests by measuring Mg melting-induced oxidation, and (2) to confirm that unburnt Mg is encapsulated in combustion products Additional experiments with pure Mg enabled comparison between heat flow behaviors and demonstration that Mg in post-bomb products is not immediately available for oxidation, unlike pure metal powders.

A Netzsch STA 449 F3 Jupiter machine was used for the DSC experiments. Powder samples of approximately 10 mg were placed in open alumina pans and positioned in the instrument chamber with a controlled environment of 80 ml/min oxygen and 20 ml/min argon. The sample was heated from room temperature up to 1000 °C at a temperature scan rate of 10 °C/min. Experiments were performed in triplicate to ensure repeatability.

2.4. X-ray Diffraction (XRD)

The post-burn powders were also characterized using a Rigaku MiniFlex II powder diffractometer. The XRD patterns were obtained by scanning a 2θ range of 5–70°, step size = 0.02°, and scan time of 2°/minute. The X-ray source was Cu Kα radiation (λ = 1.5418 Å) with an anode voltage of 30 kV and a current of 15 mA. Diffraction intensities were recorded on a position sensitive detector (D/teX Ultra). The patterns were analyzed using MDI JADE Material Data software with ICDD database.

3. Results

3.1. Combustion completeness

The measured heat of combustion, ΔH_c, of Mg powders tested by bomb calorimetry is summarized in Table 1. The combustion completeness, η, i.e., fraction of metal reacted in the calorimeter, was calculated as the ratio of the measured ΔH_c to the theoretical magnesium oxidation heat of combustion, $\Delta H_c^T = 24.73$ kJ/g [15], according to Reaction (1).

$$\mathrm{Mg} + \frac{1}{2}\mathrm{O_2} = \mathrm{MgO} \quad (1)$$

The incomplete Mg combustion is statistically evident for both tested sizes of Mg powder. For Al powder, combustion completeness is 98 ± 2 % obtained in the same experimental configuration [14]. The combustion of suspended Al powder in the bomb calorimeter is complete (within the experimental error), whereas there is measurable incomplete combustion with Mg powder.

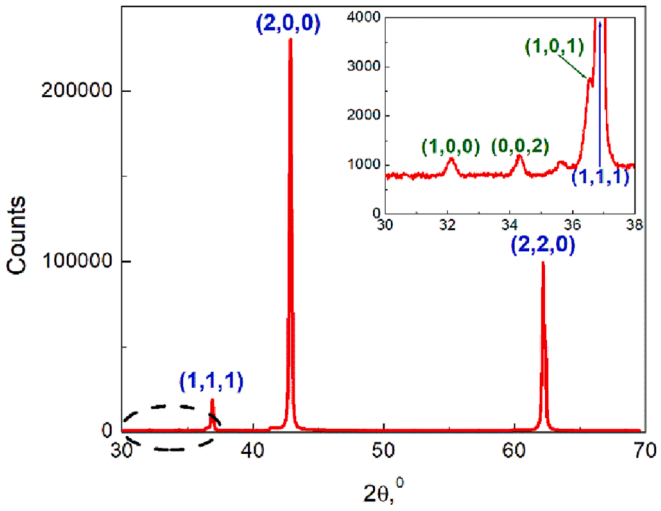

Fig. 2. The XRD pattern of combustion products of 10 μm Mg powder. The inset is an enlargement of the circled area. MgO peaks (ICDD #01-071-1176) are indexed in Blue color and Mg peaks (ICDD #01-071-3765) are indexed in Green color.

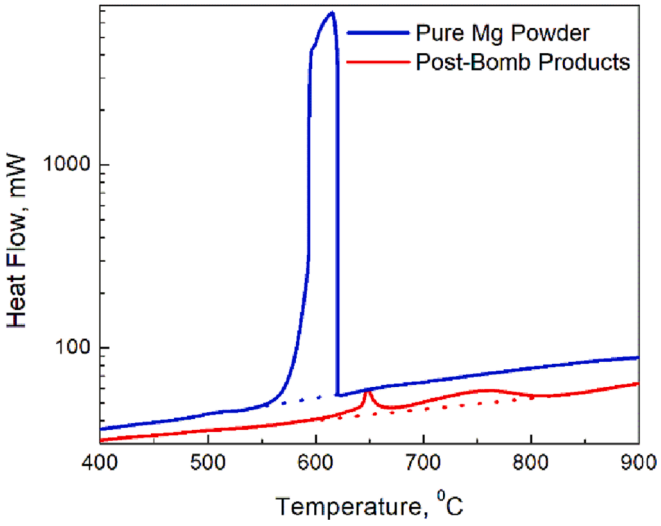

Fig. 3. Heat flow as a function of temperature for pure 100 μm Mg powder and its post-bomb combustion products in an atmosphere of 80 % O_2:20 % Ar by volume with a heating rate of 10 °C/min. Sample mass was 10 mg for both powders. Different temperature ranges of exothermic behavior (Mg oxidation) are evident. The dotted lines correspond to the DSC curves background to be subtracted in order to quantify the heat released due to Mg oxidation.

3.2. Phase composition of combustion products

The X-ray Diffraction (XRD) pattern of post-bomb products recovered after combustion of 10 μm nominal size Mg powder is shown in Fig. 2. Remnant Mg is seen together with MgO. The XRD pattern of combustion products of 100 μm nominal size Mg powder is similar confirming the presence of unburnt Mg recovered from the bomb calorimeter experiment. The trace Mg detected in the combustion products aligns with the incomplete combustion demonstrated in the bomb calorimetry tests (see Table 1).

3.3. Reactivity of post-combustion products

Results of heat flow measurements for 100 μm Mg powder and its post-bomb combustion products are shown in Fig. 3.

Table 2
Results for the remaining Mg after bomb calorimetry testing using DSC data. The average values of three DSC tests are presented with the standard deviations.

Mg Sample	10 μm	100 μm
ϕ, %	2.9 ± 0.2	4.0 ± 0.5

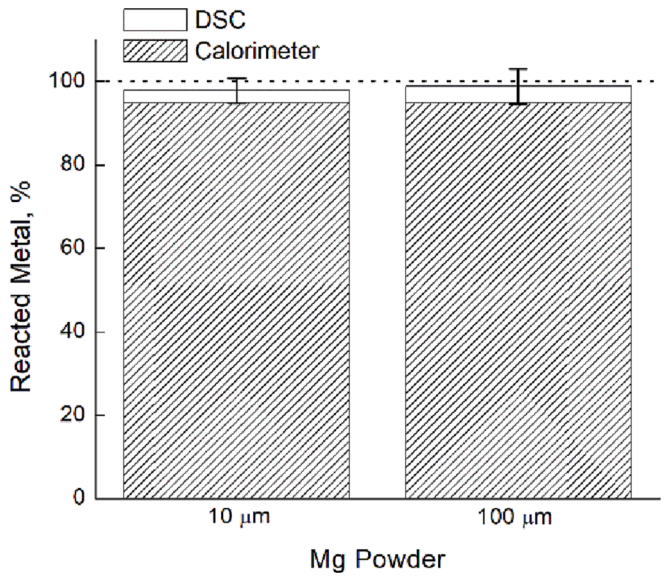

Fig. 4. Fractions of reacted metal in experiments. The dotted line (100 %) is a guide for the eye. The error bar is the sum of standard deviations of corresponding measurements.

Fig. 3 shows pre- and post-combustion powders demonstrating exothermic behavior within significantly different temperature ranges. Pure Mg powder oxidizes at lower temperatures compared with oxidation of the post-bomb combustion products. Thus, Fig. 3 provides evidence that Mg present in the post-bomb powder is not immediately available for oxidation, unlike the pure metal sample.

The Differential Scanning Calorimetry (DSC) measurements for the post-bomb products were analyzed as follows:

1. The total heat released due to Mg oxidation, ΔQ, was calculated as the area between the curve and the background (i.e., shown as a dotted line in Fig. 3).
2. The mass of Mg reacted in the DSC, m_{DSC}, was calculated using Equation (2).

$$m_{DSC} = \frac{\Delta Q}{\Delta H_c^T} \tag{2}$$

The relative fraction of Mg reacted in the DSC with respect to the total amount of metal, ϕ, was estimated using Equation (3).

$$\phi = \frac{m_{DSC}}{m_{DSC} + m_{bomb}} \bullet 100\% \tag{3}$$

In Eq. (3), the mass of Mg in the post-bomb products that was oxidized during combustion in the bomb calorimeter, m_{bomb}, is calculated from Equation (4).

$$m_{bomb} = (m_0 - m_{DSC}) \bullet \upsilon \tag{4}$$

In Eq. (4), m_0 is the mass of the post-bomb powder tested in the DSC, and the stoichiometric coefficient, υ, is defined in Equation (5).

$$\upsilon \equiv \frac{M_{Mg}}{M_{MgO}} \tag{5}$$

In Equation (5), M_{Mg} and M_{MgO} are molar masses of magnesium and magnesia (MgO), correspondingly.

Results for the remaining Mg from this analysis are summarized in Table 2.

The amount of Mg oxidized in the DSC is quantifiable. Table 2 shows Mg was not burnt to completion in the calorimeter, and the measurable Mg content is high enough to explain the incomplete Mg powder combustion seen in the bomb calorimetry tests. Fig. 4 illustrates that the combustion completeness in the calorimeter, η, and the fraction of Mg reacted in the DSC, ϕ, add to 100 % within the measurement error, which is the sum of standard deviations of corresponding measurements.

4. Discussion

4.1. Mechanism of unburnt metal encapsulation

At first glance, the combustion incompleteness on the order of 5 % found for Mg combustion in the calorimeter does not look very unusual. It can be ascribed to a metal particle extinguishing that might naturally occur at the end of combustion. The amount of unburnt metal revealed in the DSC quantitatively corresponds to the Mg combustion incompleteness and aligns with the overall energy balance. Based on the results summarized in Fig. 3, the Mg combustion incompleteness should be considered while describing the system energetic performance. Currently, numerical models are designed on the assumption of complete Mg combustion [16,17].

Another, more important question is related to the mechanism enabling incomplete Mg combustion, and the need to consider this mechanism in numerical models of metal combustion. As shown in Fig. 3, DSC heat flows for pure metal and post-bomb products demonstrate Mg oxidation at different temperatures. Post-bomb powder reacts at noticeably higher temperatures. Therefore, Mg contained in the post-bomb products is not immediately available for oxidation. Moreover, the heat flow for the post-bomb products is sharply peaking at 650 °C (see Fig. 2), which is the Mg melting temperature. Thus, the oxidation of Mg contained in the post-bomb products becomes possible only upon metal melting. This can be explained if Mg is initially encapsulated in the combustion products, i.e., the Mg core occurs within the MgO shell. Then, since the density of liquid Mg is smaller than that of solid metal (about 10 % difference) [18], upon melting Mg expands. For metal encapsulated within a relatively rigid shell, expansion leads to stress-induced breakage of the shell that is followed by molten metal infiltration through pores that appear in that stressed shell. As a result, the initially encapsulated Mg can oxidize.

The Mg encapsulation in the combustion products happens during metal particle combustion and is the direct consequence of the strict energy balance of the process [9,13]. In brief, the energy released in the volume around the burning particle is not enough to sustain the steady-state process due to the significant condense-luminescent radiative loss. Then, the partial condensation of gaseous oxides on the surface of the burning particle produces energy which compensates the radiative loss and is an essential part of the process to satisfy the energy balance. Thus, this condensation of gaseous oxides on the burning particle is a process responsible for formation of micron-sized oxide particles, which fraction in combustion products can be as much as ~10–20 % [12,13]. Due to a limited understanding of light emission during metal combustion, the energy deficit and, therefore, a need to incorporate partial condensation has not historically been given attention since seminal work on concepts of metal particle combustion [10,11].

The oxide film formed on the surface of the burning particle could ultimately extinguish combustion leading to the unburnt metal core within the grown oxide shell. However, the applicability of the latter statement, and, therefore, the occurrence of unburnt metal depends on the possibility of an interfacial condensed oxide-metal surface reaction [9,12]. In the case of Al, an interfacial reaction can be described by Equation (6),

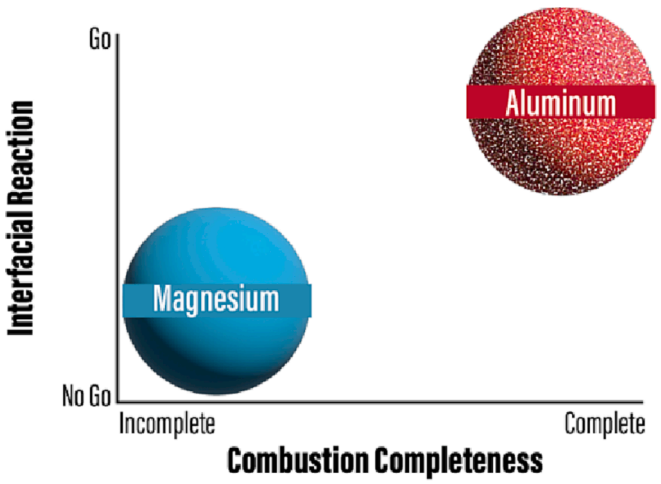

Fig. 5. The sketch illustrating the difference between Mg and Al systems in terms of relations between the interfacial reaction occurrence and combustion completeness.

$$4 \bullet \mathrm{Al(cond)} + \mathrm{Al_2O_3(cond)} = 3\bullet\mathrm{Al_2O(gas)} \quad (6)$$

and provides a mechanism of metal consumption within the oxide shell. Then, no unburnt metal is seen in Al combustion because formation of gaseous metal suboxides is thermodynamically favorable and consume the metal core.

On the contrary, in the case of Mg, a reaction similar to Equation (6) is impossible due to the magnesia properties that do not allow for multiple gaseous suboxides: the only existing gaseous oxide has the same stoichiometry as the condensed oxide, i.e., MgO. The absence of that interfacial reaction in the Mg-MgO system is the reason why unburnt metal is seen in Mg combustion. A possibility to control the nanoparticle growth [19], and, therefore, the radiative loss could help reduce or even eliminate that unburnt metal.

Fig. 5 illustrates the difference between the Mg and Al systems and shows that interfacial reactions leading to formation of gaseous suboxide help promote complete Al combustion while the impossibility of suboxide formation in the case of Mg limits complete Mg combustion.

5. Concluding remarks

Based on the analysis of Mg combustion provided in the current work, the occurrence of an unburnt metal core within the oxide shell in the combustion products is demonstrated. The quantified incompleteness of Mg combustion is an inherent peculiarity of its combustion process and is about 5 %. The reason of the unburnt Mg core is unique for this metal and does not occur in the case of Al combustion.

The mechanism that enables the formation of the unburnt metal core within the oxide shell in the case of Mg combustion is related to the partial condensation of gaseous oxides on the surface of the burning metal particle. This gaseous oxide condensation is essential for the overall energy balance of burning metal particles, and it is not limited to the Mg case only. Inclusion of fundamental processes such as energy from the partial condensation of gaseous oxides on the burning particle surface is required for consistent modeling and predictive performance. But in the case of Mg, interfacial reactions between the encapsulating oxide product residue and metal is impossible due to the specific stoichiometry that traps unburnt Mg from continued oxidation.

The reason of the unburnt metal occurrence is related to the condense-luminescent radiative loss during formation of nano-oxides. A possibility to control the nanoparticle growth and radiative loss could help reduce unburnt metal. As a result, the potential for metal-based propulsion would be extended. The physics of condense-luminescence and ability to control energy exchange processes in the design of metal fuels will reduce unburnt metal and increase energy generating capabilities.

CRediT authorship contribution statement

Quan Tran: Investigation, Data curation. **Neil Vaz:** Investigation, Data curation. **Michelle L. Pantoya:** Methodology, Supervision, Writing – review & editing. **Igor Altman:** Conceptualization, Methodolog, Formal analysis, Writing – original draft.

Declaration of Competing Interest

The authors declare that they have no known competing financial interests or personal relationships that could have appeared to influence the work reported in this paper.

Data availability

Data will be made available on request.

Acknowledgements

The authors from TTU (QT, NV, MP) are grateful for support from United States Office of Naval Research (ONR) grant number N00014-22-2006 and Dr. Chad Stoltz, and STEM grants N00014-21-2519 and NA0003988. Also, IA is thankful for funding from the NAVAIR ILIR program managed at the ONR and administered by Dr. Alan Van Nevel.

References

[1] Price EW, Sigman RK. Combustion of aluminized solid propellants. In: Yang V, Brill TB, Ren WZ, editors. Solid propellant chemistry, combustion, and motor ballistics. New York: AIAA; 2000. p. 663–87.
[2] Sundaram D, Yang V, Yetter R. Metal-based nanoenergetic materials: synthesis, properties, and applications. Prog Energy Combust Sci 2017;61:293–365.
[3] Sandall EricT, Kalman J, Quigley JN, Munro S, Hedman TD. A study of solid ramjet fuel containing boron–magnesium mixtures. Propul Power Res 2017;6(4):243–52.
[4] Belal H, Han CW, Gunduz IE, Ortalan V, Son SF. Ignition and combustion behavior of mechanically activated Al–Mg particles in composite solid propellants. Combust Flame 2018;194:410–8.
[5] Shafirovich E, Varma A. Metal-CO_2 propulsion for mars missions: current status and opportunities. J Propul Power 2008;24(3):385–94.
[6] Trent DJ, Thomas HD, Rucker MA. Updated Human Mars Ascent Vehicle concept in support of NASA's strategic analysis cycle 2021. In: 2022 IEEE Aerospace Conference (AERO), Big Sky, MT, USA; 2021. p. 1–13. https://doi.org/10.1109/AERO53065.2022.9843319.
[7] Li M, Hu C, Wang Z, Li Y, Hu J, Hu X, et al. Application and performance estimation of Mg/CO_2 engine on Mars. Acta Astronaut 2022;192:314–27.
[8] Wang X, Bu Y, Xu X, Yang Q. Experimental investigation on the thrust regulation of a Mg–CO_2 Martian ramjet. Acta Astronaut 2022;197:191–9.
[9] Altman I, Pantoya M. Comprehending metal particle combustion: A path forward. Propellants Explos Pyrotech 2022;47:e202200040.
[10] Brzustowski T, Glassman I. Spectroscopic investigation of metal combustion. In: Wolfhard H, Glassman I, Green L, editors. Heterogeneous combustion. New York: Academic Press; 1964. p. 41–74.
[11] Klyachko LA. Combustion of a stationary particle of low-boiling metal. Combust Explos Shock Waves 1969;5(3):279–84.
[12] Tran Q, Pantoya ML, Altman I. Condense-luminescence and global characterization of metal particle suspension combustion. Appl Energy Combust Sci 2022;11:100080.
[13] Altman I, Vovchuk Y. Thermal regime of the vapor-state combustion of magnesium particle. Combust Explos Shock Waves 2000;36:227–9.
[14] Tran Q, Altman I, Dube P, Malkoun M, Sadangi R, Koch R, et al. Direct demonstration of complete combustion of gas-suspended powder metal fuel using bomb calorimetry. Meas Sci Technol 2022;33(4):047002.
[15] NIST Chemistry WebBook, available at <https://webbook.nist.gov> (retrieved September 20, 2022).
[16] Maghsoudi P, Bidabadi M. Analytical and numerical evaluation of flammability limit of magnesium-fueled thermophotovoltaic combustor considering inter-regional radiation, heat loss and O2–N2, Ar, He oxidizers. Fuel 2022;312:122848.
[17] Maghsoudi P, Bidabadi M. Particle trajectory and pulsation flame of magnesium combustion. Fuel 2023;338:127230.
[18] Handbook of inorganic chemicals by P. Patnaik. McGraw-Hill, New York, 2003.
[19] Altman I, Fomenko E, Agranovski IE. Fundamental insight into critical phenomena in condensation growth of nanoparticles in a flame. Sci Rep 2022;12:15699.